Growth and Structural Characterisation of V/Fe Multilayers

A. Marczyńska, J. Skoryna, B. Szymański* and L. Smardz

Institute of Molecular Physics, Polish Academy of Sciences, M. Smoluchowskiego 17, 60-179 Poznań, Poland

The (110) oriented V/Fe multilayers were prepared at room temperature using UHV magnetron sputtering. As a substrate we have used Si(100) wafers with an oxidised surface. The surface chemical composition and the cleanness of all layers was checked *in situ*, immediately after deposition, transferring the samples to an UHV analysis chamber equipped with X-ray photoelectron spectroscopy. The structure of the multilayers has been studied *ex situ* by low- and high-angle X-ray diffraction. The modulation wavelength was determined from the spacing between satellite peaks in the X-ray diffraction patterns. Results were consistent with the values obtained from total thickness divided by the number of repetitions. Growth of the Fe (V) on 1.6 nm V (Fe) underlayer was studied by succesive deposition and X-ray photoelectron spectroscopy measurements starting from 0.2 nm of Fe (V) layer, respectively. From the exponential variation of the X-ray photoelectron spectroscopy Fe $2p$ and V $2p$ integral intensities with increasing layer thickness we conclude that the Fe and V sublayers grow homogeneously in the planar mode.

1. Introduction

Metallic multilayers (MLs) composed of alternating sublayers of ferromagnetic and non-magnetic metals has attracted great interest over the past years because of the successful application of these materials as ultrasensitive hard disc reading heads and magnetic sensors [1, 2]. Furthermore, V(001)/Fe(001) MLs were used very recently as a model system to study finite size effect [3]. However, for such MLs only "long period" (0.8–1.0 nm) of antiferromagnetic (AFM) interlayer coupling was found [4, 5]. The first peak of AFM coupling was observed for vanadium layer thickness between 2 [4] and 2.2 nm [5] instead expected $d_V = 1.2$ nm. The above behaviour was explained by magnetic polarisation of V atoms near V–Fe and Fe–V interfaces. On the other hand, for nearly perfect Fe(100) substrates and high quality Fe/Cr interfaces, "short period" AFM coupling between Fe(100) films separated by Cr was observed [6]. Imperfect interfaces, however, can suppress the short period coupling between Fe layers [6].

In general, the magnetic properties of MLs can be tailored by varying the composition, thickness and microstructure of the magnetic and non-magnetic sublayers. The strength and sign of the interlayer exchange coupling could be tuned by alloying the spacer with nonmagnetic elements [7] or using hydrogen [8, 9]. In the later case it could be changed not only by electronic structure but also by thickness of the spacer.

For the (001) oriented V/Fe MLs, there is extensive literature on the growth and structural characterisation [4, 5, 7–9]. Much less work has focused on preparation and characterisation of (110) oriented V/Fe MLs. In this paper we report on growth and structure of

V(110)/Fe(110) MLs using *in situ* X-ray photoelectron spectroscopy (XPS) and *ex situ* standard $\theta - 2\theta$ X-ray diffraction (XRD), respectively.

2. Experimental details

The V/Fe multilayers were prepared at room temperature (RT) using computer-controlled ultra high vacuum (UHV) magnetron sputtering [10]. The number of repetitions of the base period was equal to 25. A capping layer of 5 nm Pd was used to allow a fast uptake and release of hydrogen at a temperature of less than 370 K and to avoid oxidation of the MLs. As a substrate we have used Si(100) wafers with an oxidised surface to prevent a silicide formation [11]. Therefore we have applied a special heat treatment in UHV before deposition in order to obtain an epitaxial SiO_2 surface layer [11, 12]. The Fe-layers ($0 < d_{Fe} < 11$ nm) were deposited using a DC source. For preparation of the V-layers ($0 < d_v < 11$ nm) an RF source was used. In the case of V/Fe MLs a 1.6 nm V buffer layer was first deposited to enhance the (110) growth.

The chemical composition and the cleanness of all layers were checked *in situ*, immediately after deposition,
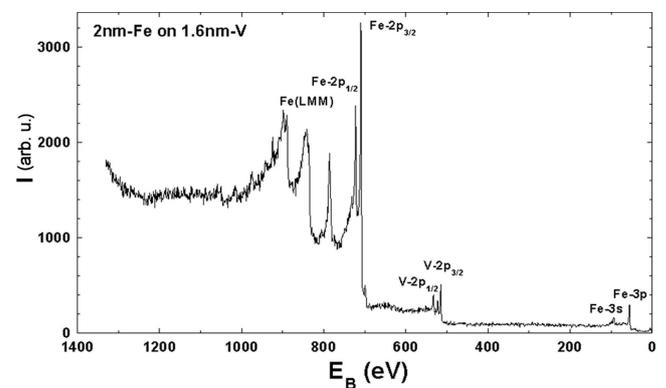
Fig. 1. XPS (Al K_α) core-level spectrum of freshly deposited 2 nm Fe layer on 1.6 nm thick vanadium.

*corresponding author; e-mail: szyman@ifmpan.poznan.pl

transferring the samples to an UHV analysis chamber equipped with XPS, Auger electron spectroscopy (AES) and ion gun etching system. The XPS core level spectra were measured with Al K_α radiation at 1486.6 eV at RT using a SPECS EA 10 PLUS energy spectrometer. Details of the XPS measurements can be found in Ref. [13].

The morphology and roughness of the Pd capping layers were studied *ex situ* by atomic force microscopy (AFM). The structure of the V/Fe MLs was examined *ex situ* by standard $\theta - 2\theta$ XRD with Cu K_α radiation. The modulation wavelength was determined from the spacing between satellite peaks in the high- and low-angle X-ray diffraction patterns. The thicknesses of individual Fe and V sublayers were also determined using X-ray fluorescence analysis (XRF).

3. Results and discussion

The chemical composition and the cleanness of all layers were revealed *in situ*, immediately after deposition, by XPS. In Fig. 1 we show XPS spectrum of 1 nm Fe overlayer deposited on 1.6 nm V underlayer. As can be observed in Fig. 1, practically no XPS signals were observed from O $1s$ or C $1s$ and any other potential contaminations.

In the XPS experiment we have also studied the Fe layer growth on a 1.6 nm V underlayer. The freshly deposited 1.6 nm V/d_0 Fe bilayer was *in situ* transferred from the preparation chamber (5×10^{-10} mbar) to the analysis chamber(5×10^{-11} mbar), where the XPS Fe $2p$ and V $2p$ core level spectra were immediately measured in vacuum of 8×10^{-11} mbar. Then the bilayer was transferred back to the preparation chamber and the deposition process of the Fe overlayer was continued. The above procedure (overlayer deposition and XPS core level measurements) was repeated until the Fe $2p_{3/2}$ and V $2p_{3/2}$ integral intensities were saturated. Practically no trace of oxygen (or any other contaminations) adsorption or surface oxide formation was detected during the transfer operation or XPS measurements ($\approx$10 min).

In Fig. 2 we show XPS core-level spectra measured for Fe $2p_{3/2}$ and Fe $2p_{1/2}$ (Fig. 2a), and V $2p_{3/2}$ and V $2p_{1/2}$ (Fig. 2b) peaks for the 1 nm Fe layer deposited on 1.6 nm vanadium underlayer. The positions and the exchange splitting between $2p_{3/2}$ and $2p_{1/2}$ peaks are practically the same compared to those measured for bulk materials.

According to the XPS theory [14] the XPS integral intensities for intense $2p_{3/2}$ peaks of the top Fe (I_0) and bottom V (I_s) layer for the planar growth are described by

$$I_0 = I_0^\infty \left(1 - \mathrm{e}^{-d_0/L}\right), \quad I_s = I_s^\infty \mathrm{e}^{-d_0/L}, \qquad (1)$$

where d_0 and L denote the overlayer thickness and escape depth of the excited photoelectrons, respectively. After transformations of Eqs. (1), the ideal planar growth of a bilayer system with perfectly sharp interface is represented by a linear equation

$$\ln\left[(I_s + I_0)/I_s\right] = d_0/L. \qquad (2)$$

The perfectly planar growth of the model bilayer system [14] is represented by the bold solid line in Fig. 3.
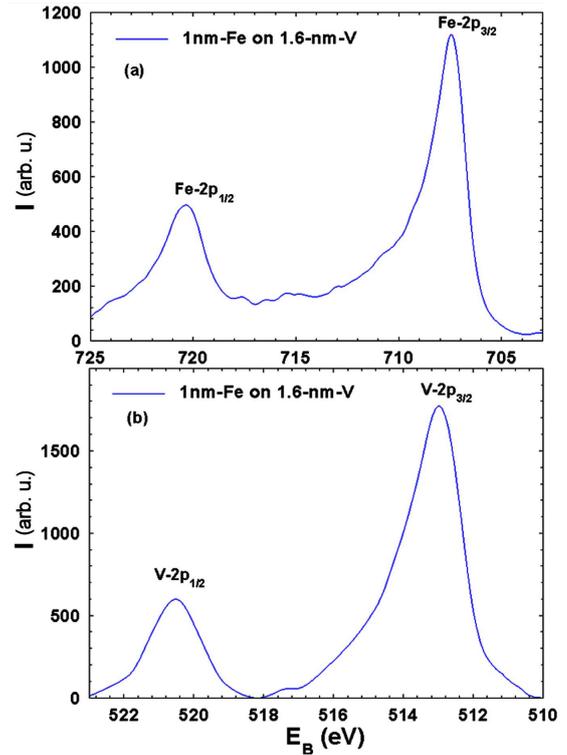
Fig. 2. XPS (Al K$_\alpha$) spectrum of Fe $2p$ (a) and V $2p$ peaks measured for *in-situ* freshly prepared 1 nm Fe layer on 1.6 nm vanadium.
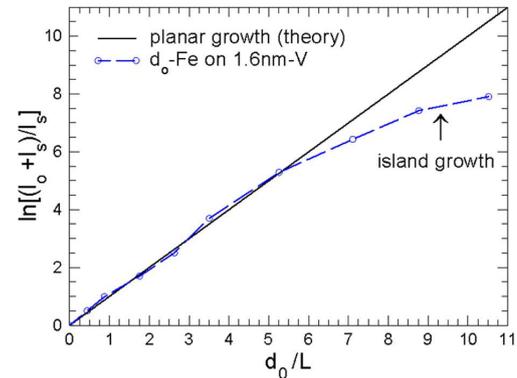
Fig. 3. $\ln((I_S + I_0)/I_S)$ as a function of d_0/L (see text). Solid line denotes theoretical (without interface mixing) planar growth of the overlayer [14]. Thin broken lines (open circles connected with broken line) represent linear fit to the experimental data.

Our experimental results (open circles) can be also fitted by linear regressions (see Fig. 3) but only up to Fe layer thickness of about 5 nm, which reveals planar growth (solid line in Fig. 3). For the calculation of the d_0/L ratio we have taken escape depth values of $L_{\mathrm{Fe}\ 2p} = 1.15$ nm and $L_{\mathrm{V}\ 2p} = 1.3$ nm [14]. The reason for the significantly lower slope of the experimental data shown in Fig. 2 above Fe layer thickness greater than 5 nm is the island growth during the deposition process [14–16]. We have observed very similar behaviour

during V growth on 1.6 nm Fe underlayer. From the exponential variation of the XPS Fe $2p$ and V $2p$ integral intensities with increasing overlayer Fe (V) thickness up to 5 nm we conclude that the Fe and V sublayers grow homogeneously in the planar mode [14]. We have previously observed very similar growth mode for Fe/Ti [15] and Fe/Zr [16] bilayers.
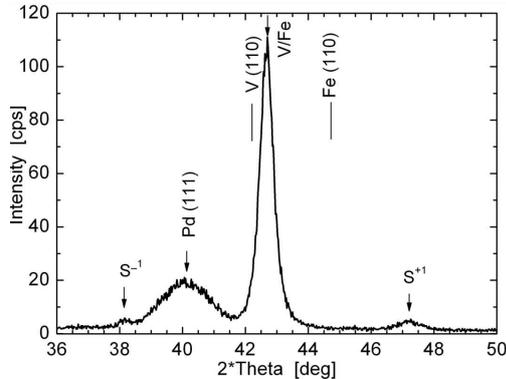
Fig. 4. High-angle $\theta - 2\theta$ XRD (Cu K$_\alpha$) pattern for the 1 nm V/0.6 nm Fe multilayer.

The structural quality of the multilayers was characterized by high- and low-angle XRD. Figure 4 presents high-angle diffraction data taken from multilayered sample of 1 nm V/0.6 nm Fe having 25 bilayer periods. The spectrum shows only diffraction peaks associated with the (110) bcc iron and (110) bcc vanadium planes revealing strong preferential growth in direction perpendicular to the substrate. For all the samples we have observed central Bragg peak (CBP) located between positions expected for reflections of bcc Fe(110) and bcc V(110) and at least two satellites for the MLs with the thinner sublayers (see Fig. 4). The fitted roughness from the low-angle data was about 0.3–0.4 nm, which is in agreement with AFM measurements [17]. The modulation of composition of the V/Fe MLs was also confirmed in the low-angle XRD patterns by intense satellite peaks. The wavelengths of modulation calculated from the high- and low-angle satellite peaks were in good agreement with those values determined from XRF.

In conclusion, the planar growth of the Fe and V sublayers was confirmed *in situ* by XPS measurements. The arifical superstructure and prefered (110) orientation were revealed by XRD experiment.

References

[1] A. Barthélémy, A. Fert, J-P. Contour, M. Bowen, V. Cros, J.M. De Teresa, A. Hamzic, J.C. Faini, J.M. George, J. Grollier, F. Montaigne, F. Pailloux, F. Petroff, C. Vouille, *J. Magn. Magn. Mater.* **242-245**, 68 (2002).

[2] S.A. Wolf, D.D. Awschalom, R.A. Buhrman, J.M. Daughton, S. von Molnár, M.L. Roukes, A.Y. Chtchelkanova, D.M. Freger, *Science* **294**, 1488 (2001).

[3] Xiao Xin, G. Pálsson, M. Wolff, B. Hjörvarsson, *Phys. Rev. Lett.* **113**, 046103 (2014).

[4] M. Ahlberg, E.T. Papaioannou, G. Nowak, B. Hjörvarsson, *J. Magn. Magn. Mater.* **341**, 142 (2013).

[5] M.M. Schwickert, R. Coehoorn, M.A. Tomaz, E. Mayo, D. Lederman, W.L. O'Brien, Tao Lin, G.R. Harp, *Phys. Rev. B* **57**, 13681 (1998-I).

[6] D.T. Pierce, J.A. Stroscio, J. Unguris, R.J. Celotta, *Phys. Rev. B* **49**, 14565 (1994).

[7] B. Skubic, E. Holmström, D. Iusan, O. Bengone, O. Eriksson, R. Brucas, B. Hjörvarsson, V. Stancu, P. Nordblad, *Phys. Rev. Lett.* **96**, 057205 (2006).

[8] F. Klose, Ch. Rehm, D. Nagengast, H. Maletta, A. Weindinger, *Phys. Rev. Lett.* **78**, 1150 (1996).

[9] B. Hjörvarsson, J.A. Dura, P. Isberg, T. Watanabe, T.J. Udovic, G. Andersson, C.F. Majkrzak, *Phys. Rev. Lett.* **79**, 901 (1997).

[10] L. Smardz, *Solid State Commun.* **112**, 693 (1999).

[11] See for example, *The Physics and Chemistry of SiO$_2$ and the Si-SiO$_2$ Interface*, Eds. C.R. Helms, B.E. Deal, Plenum, New York 1988.

[12] L. Smardz, U. Köbler, W. Zinn, *J. Appl. Phys.* **71**, 5199 (1992).

[13] L. Smardz, M. Jurczyk, M. Nowak, *Int. J. Hydrogen En.* **37**, 3659 (2012).

[14] D. Briggs, in: *Handbook of X-Ray and Ultraviolet Photoelectron Spectroscopy*, Ed. D. Briggs, Heyden, London 1977, p. 153.

[15] L. Smardz, K. Smardz, H. Niedoba, *Phys. Status Solidi B* **243**, 227 (2006).

[16] L. Smardz, K. Smardz, *Mater. Sci.-Poland* **24**, 821 (2006).

[17] J. Skoryna, A. Marczyńska, M. Lewandowski, L. Smardz, *J. Alloy Comp.* in print (2015).